

EFFECT OF CHEMICAL PRE-TREATMENTS ON THE STABILITY OF MELT-SPUN $Mg_{50}Ni_{30}Y_{20}$ IN EXTREME ALKALINE ELECTROLYTE

A. Gebert, B. Khorkounov and L. Schultz

Leibniz- IFW Dresden, P.O. Box: 270016, 01171 Dresden, Germany

Received: March 29, 2008

Abstract. Melt-spun amorphous-nanocrystalline $Mg_{50}Ni_{30}Y_{20}$ samples were subjected to chemical pre-treatments in 1% HF and in 10 mg/l YCl_3 /1% H_2O_2 solution. Their electrochemical behavior in the as-quenched state and after hydrogen charging at -5 mA/cm^2 for 20 hours was studied in 6 M KOH, pH=14,8, by means of potentiodynamic polarisation measurements. A pre-treatment with HF solution can improve their anodic passivation behavior by inhibiting a preferential nickel oxidation-dissolution at low polarisation, whereas a YCl_3 / H_2O_2 solution treatment has the opposite effect. Both pre-treatment methods lead to an enhancement of cathodically induced surface degradation processes.

1. INTRODUCTION

In the development of new hydrogen absorbing materials for metal hydride electrodes of rechargeable Ni-MH batteries [1] nanocrystalline and amorphous Mg-Ni- based alloys in close relation to the Mg_2Ni compound (with theoretical $C_{max} = 1000 \text{ mAh/g}$ corresponding to the formation of Mg_2NiH_4 [2]) find currently special attention. Though first studies on electrodes made from those powders are promising with respect to the practically attained discharge capacities, one of the major problems is the low corrosion resistance at $pH > 14$, which strongly limits the cycle life stability [3,4]. Various approaches have been followed for improving the cycle life of Mg-Ni- based electrodes. Besides compositional modifications – mainly with transition metals or rare earths, preparation of composite materials and particle size control also chemical surface modifications are regarded a useful ways [5]. Recently we investigated fundamentally the corrosion behaviour of rapidly quenched and hydrogenated $Mg_{50}Ni_{30}Y_{20}$ and $Mg_{63}Ni_{30}Y_7$ samples in alkaline environments [6]. Increased yttrium con-

tent of the alloy was found to be beneficial for inhibiting a preferential anodic nickel dissolution from the surface prior to and after cathodic hydrogenation.

In the present paper, investigations on the effect chemical pre-treatment methods are described. A treatment in acidic to alkaline fluoride solutions can lead to selective component dissolution or to the formation of stable salt layers [7,8]. The formation of a conversion coating of $Y(OH)_3$ / Y_2O_3 is anticipated by exposure in YCl_3/H_2O_2 [9].

2. EXPERIMENTAL

Amorphous-nanocrystalline $Mg_{50}Ni_{30}Y_{20}$ samples were produced by melt-spinning. Details of preparation and microstructure characterization are described in [6]. Ribbon samples were exposed for 30 sec in a 1% HF solution, then dried in air. The conversion coating was formed by repeated dipping in 10 mg/l YCl_3 /1% H_2O_2 solution (6 x 30 sec) and drying in air. The surface modifications were examined using optical microscopy (OM), scanning electron microscopy (SEM with EDX) and atomic

Corresponding author: A. Gebert, e-mail: gebert@ifw-dresden.de

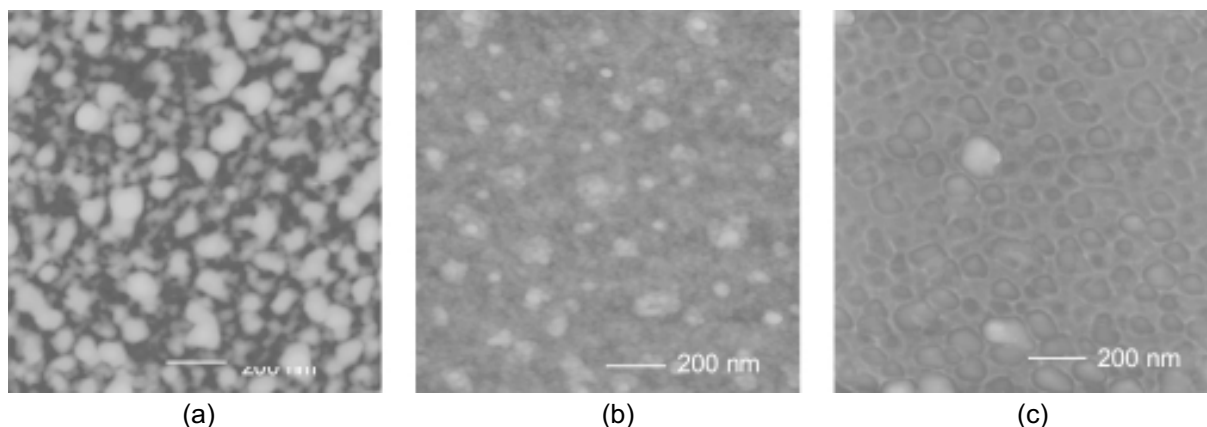


Fig. 1. AFM images of $\text{Mg}_{50}\text{Ni}_{30}\text{Y}_{20}$ ribbon surfaces (upper side) in the as-quenched state (1a), after treatment in 1% HF solution (1b), and in 10 mg/l YCl_3 / 1% H_2O_2 solution (1c) (depth : 30 nm).

force microscopy (AFM). Electrochemical studies were performed in 6M KOH solution, $\text{pH} = 14,8$, N_2 -purged, using a Solartron SI 1287 Electrochemical Interface connected to a cell with Pt counter and SCE reference electrode. Slow polarization measurements at a scan-rate of 0,5 mV/s as well as cyclic polarization tests at a scan-rate of 5 mV/s were conducted. Hydrogen pre-charging was performed at $i = -5 \text{ mA/cm}^2$ for 20 hours. The hydrogen content [H] was determined using hot gas extraction. All tests were performed 2-3 times to ensure reliability of the data.

3. RESULTS AND DISCUSSION

In the as-quenched state the $\text{Mg}_{50}\text{Ni}_{30}\text{Y}_{20}$ ribbon surface appears macroscopically smooth except some crystalline defects, their occurrence can not be avoided under the given preparation conditions [6]. However, on the sub-micron scale the surface topography is quite rough (Fig. 1a) corresponding to the amorphous-nanocrystalline microstructure. A thick porous coarse-grained coating is formed after the $\text{YCl}_3/\text{H}_2\text{O}_2$ solution treatment. SEM-EDX analysis revealed yttrium and oxygen species as main coating components. This layer was stable also after 24 hours exposure in 6M KOH solution. In contrast, the HF treatment did not macroscopically modify the ribbon surface. AFM imaging of the ribbon surface after HF treatment and after $\text{YCl}_3/\text{H}_2\text{O}_2$ solution treatment and subsequent careful removal of the coating (Figs. 1b and 1c) revealed

in both cases a significant change in the surface topography as compared to the as-quenched state. This indicates that not only naturally formed passive films are removed, but that also the alloy surface is attacked in terms of selective component dissolution causing a transformation of the surface state with residual component species.

Slow anodic polarisation curves of as-quenched and chemically pre-treated ribbons were recorded in 6M KOH (not shown here). Due to the main fraction of highly reactive components magnesium and yttrium the corrosion potential of the untreated alloy establishes at a quite negative potential, $U_{\text{corr}} = -0.9 \text{ V}$, which is close to the equilibrium potential for the hydrogen reduction and corresponds to a current density $i_{\text{corr}} = 0.5 \mu\text{A/cm}^2$. Upon anodic polarisation a stable passive state is attained with passive current densities in the range of $i_{\text{pass}} \sim 3 \text{ mA/cm}^2$. The HF treatment leads to an even more reactive state under low polarisation conditions according to a negative shift of U_{corr} by about 100 mV (see also Fig. 2) and slightly increased corrosion current densities. But under anodic conditions decreased passive current densities indicate the formation of somewhat more protective surface films. In contrast, after the $\text{YCl}_3/\text{H}_2\text{O}_2$ solution treatment the corrosion potential is more positive by about 80 mV, but anodic current densities are slightly increased as compared to the as-quenched state. In order to make oxidation processes clearer visible, fast cyclic polarisation measurements were

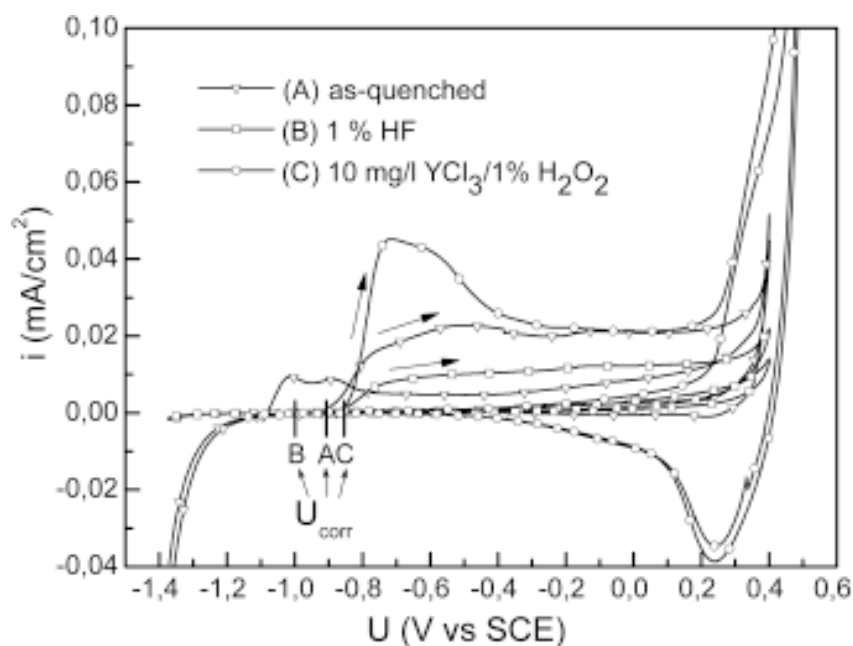


Fig. 2. Cyclic potentiodynamic polarization curves of $Mg_{50}Ni_{30}Y_{20}$ samples in the as-quenched state and after treatment in 10 mg/l YCl_3 /1% H_2O_2 solution and 1% HF solution in 6M KOH (2 cycles beginning from U_{corr} in anodic direction).

conducted, as shown Fig. 2. Comparative polarisation tests on the pure single components revealed that the anodic current flow in the first and second cycle at low anodic potentials is mainly related to the nickel oxidation. Under free and low anodic polarisation conditions $Mg(OH)_2$ and $Y(OH)_3$ can spontaneously form as thin permeable films on the untreated alloy surface. Ni anodically oxidizes initially under preferential formation soluble species, nickelite ions $HNiO_2^-$, thus being depleted from the alloy surface. Only upon further anodization solid nickel oxide species contributing to passivation can form by stepwise transformation to $Ni(OH)_2$ to Ni_3O_4 to Ni_2O_3 to NiO_2 [10]. With progressing anodic polarisation the formation of $Mg(OH)_2$ and $Y(OH)_3$ is enhanced and governs the growth of a stable protective passive film at high potentials and in particular after the second cycle [6]. The HF treatment, which activates the as-quenched ribbon surface probably by selective removal of nickel from surface-near regions, which would explain the strong negative shift of the corrosion potential, obviously supports the following anodic alloy passivation according to an inhibited nickel oxidation-dissolution at low potentials. In

result, lower anodic current densities indicate a higher protective passive state. In contrast, the thick, coarse-grained conversion coating formed by YCl_3/H_2O_2 solution treatment is not effective in improving the passivation ability of the alloy, but rather leads to enhanced anodic nickel oxidation. It is assumed that this treatment may also dissolve yttrium (and magnesium) species from the alloy surface, which are subsequently used for the built up of the ineffective conversion layer. This can cause an enrichment of nickel species underneath this porous layer, which would explain the observed positive shift of the corrosion potential and the enhanced nickel oxidation as compared to the non-treated case. Surface analytical studies by means of AES are in progress to verify this argumentation.

The chemical pre-treatments do not significantly affect the rate of the cathodic hydrogen reduction reaction, and the hydrogen uptake during cathodic charging, which was in the range of 1.2 – 1.3 wt.% for all alloy samples after 20 hours of galvanostatic polarisation. Fig. 3 shows cyclic polarisation curves after the cathodic pre-charging and subsequent readjustment of the corrosion potential for 30 min-

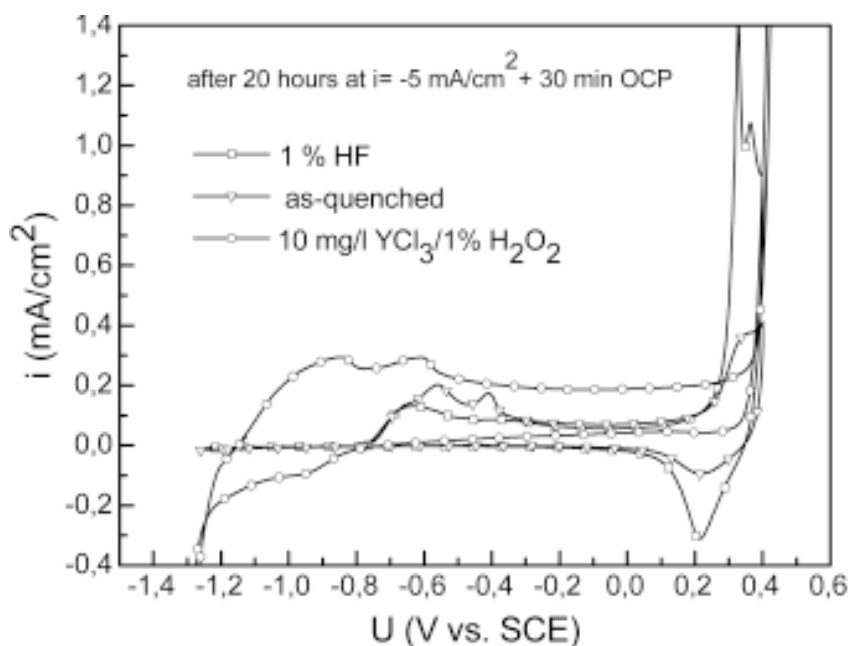


Fig. 3. Cyclic potentiodynamic polarization curves of $\text{Mg}_{50}\text{Ni}_{30}\text{Y}_{20}$ samples in 6M KOH after galvanostatic cathodic charging for 20 hours and readjustment of the corrosion potential for 30 min (1 cycle beginning from U_{corr} in anodic direction).

utes under nitrogen-purging. The overall current density level is one order of magnitude higher than that of polarisation curves shown in Fig. 2 indicating a more reactive state of the hydrogenated samples. The cathodic loading causes the formation of “active nickel” and metastable nickel hydrides at the ribbon surface, which are stepwise oxidized during the following anodic polarisation [6]. From Fig. 3 it is clearly obvious that after both chemical pre-treatments the anodic peaks for the oxidation of those species are more pronounced. It is in particular the case for the $\text{YCl}_3/\text{H}_2\text{O}_2$ -treated sample exhibiting strong peaks for the nickel hydride oxidation ($\sim -0.85 \text{ V}$), the Ni_3O_4 formation ($\sim -0.6 \text{ V}$) and the transformation to NiO_2 ($\sim 0.2 \text{ V}$). This is a similar tendency as observed for the non-charged $\text{YCl}_3/\text{H}_2\text{O}_2$ -treated sample (Fig. 2) and indicates that this treatment is very effective in triggering the enrichment of nickel species at the surface by removal/consumption of magnesium and yttrium from surface-near alloy regions. This suggests that those chemically generated surface modifications are not effective in inhibiting cathodic alloy degradation processes, but rather support them. The porous conversion coating was stable

throughout the cathodic charging and following cyclic polarisation.

4. SUMMARY AND CONCLUSIONS

A pre-treatment of melt spun amorphous-nanocrystalline $\text{Mg}_{50}\text{Ni}_{30}\text{Y}_{20}$ alloy samples with low concentrated HF solution can improve their anodic passivation ability by inhibiting nickel oxidation-dissolution at low polarisation, whereas a $\text{YCl}_3/\text{H}_2\text{O}_2$ solution treatment has the opposite effect. However, those effects are only marginal for samples in the as-quenched state. Both pre-treatments lead to an enhancement of cathodically induced surface degradation processes. In conclusion, these chemical surface modification methods are not beneficial for remarkably improving the corrosion resistance of this alloy. Other techniques, e.g. addition of further alloying additives or physically generated coatings may be more prospective.

ACKNOWLEDGEMENT

The financial support of the German Research Foundation (DFG) under grant no. Ge 1106/3 is gratefully acknowledged.

REFERENCES

- [1] K. Hong // *J. Alloys Comp.* **321** (2001) 307.
- [2] J.J. Reilly // *Z. Phys. Chemie NF* **117** (1979) 155.
- [3] Y. Hatano, T. Tachikawa, D. Mu, T. Abe, K. Watanabe and S. Morozumi // *J. Alloys Comp.* **330-332** (2002) 816.
- [4] B. Khorkounov, A. Gebert, Ch. Mickel and L. Schultz // *J. Alloys Comp.* **416** (2006) 110.
- [5] C. Rongeat, M.-H. Grosjean, S. Riggeri, M. Dehmas, S. Bourlot, S. Marchotte and L. Roue // *J. Power Sources* **158** (2006) 747.
- [6] A. Gebert, B. Khorkounov, U. Wolff, Ch. Mickel, M. Uhlemann and L. Schultz // *J. Alloys Comp.* **419** (2006) 319.
- [7] *Gmelins Handbuch für Anorganische Chemie, Magnesium Teil A* (Verlag Chemie GmbH, Weinheim, 1952), p. 790.
- [8] F.-J. Liu and S. Suda // *J. Alloys Comp.* **232** (1996) 212.
- [9] M. Dabala, K. Brunelli, E. Napoletani and M. Magrini // *Surf. Coat. Technol* **172** (2003) 227.
- [10] M. Pourbaix, *Atlas of Electrochemical Equilibria in Aqueous Solutions* (Pergamon, Press Oxford, 1966).